Available online at www.sciencedirect.com
SCIENCE DIRECT
Bioorganic & Medicinal Chemistry Letters 16 (2006) 607–614
Bioorganic & Medicinal Chemistry Letters

Characterization of high molecular weight impurities in synthetic phosphorothioate oligonucleotides

Christine Kurata, Kym Bradley, Hans Gaus, Nhuy Luu, Isaiah Cedillo, Vasulinga T. Ravikumar, Kent Van Sooy, James V. McArdle and Daniel C. Capaldi*

Isis Pharmaceuticals Inc., 1896 Rutherford Road, Carlsbad, CA 92008, USA

Received 22 September 2005; revised 13 October 2005; accepted 14 October 2005
Available online 7 November 2005

Abstract—Phosphorothioate oligonucleotides manufactured by standard phosphoramidite techniques using 2′-deoxyadenosine- or 2′-*O*-(2-methoxyethyl)-5-methylcytosine-loaded solid supports contain branched impurities consisting of two chains linked through the exocyclic amino group of the 3′-terminal nucleoside of one chain and the 3′-terminal hydroxyl group of another via a P(O)SH group. These impurities are not produced when a universal, non-nucleoside derivatized support is used.

Synthetic oligonucleotides are widely used in molecular biology and diagnostics. Recently, DNA and RNA analogs have emerged as potential drugs for treatment of diseases through antisense mechanisms of action.[1–4] The most advanced drug candidates are phosphorothioate oligonucleotides (PS-oligonucleotides) in which one of the non-bridging oxygens of the phosphate diester internucleotide linkage of DNA or RNA is replaced by sulfur. Automated synthesis of oligonucleotides is normally accomplished by addition of commercially available nucleoside phosphoramidites to a growing oligonucleotide anchored at its 3′-end to a solid support.[5] The development of improved methods for the manufacture of therapeutic-grade oligonucleotides remains an area of intense research.[6–12] Over the course of our experience in the manufacture of PS-oligonucleotides by the solid phase phosphoramidite approach, we routinely observed the occurrence of what appeared to be very high molecular weight impurities. These components were especially prominent in sequences possessing 3′-terminal adenine or cytosine heterocycles. In this report, we describe the structure elucidation of these impurities, suggest a mechanism of formation, and provide a means for their avoidance.

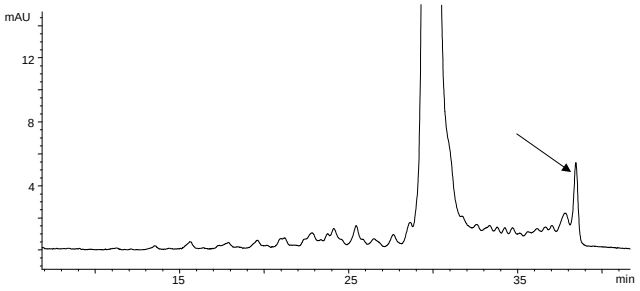

Figure 1. HPLC–UV chromatogram of RP-HPLC purified ISIS 3521.

ISIS 3521 is a 2′-deoxy PS-oligonucleotide, the nucleotide sequence of which is shown here: PS-d(GTTCTC GCTGGTGAGTTTCA).[13] The HPLC–UV chromatogram of a typical batch of reversed phase RP-HPLC purified ISIS 3521 is shown in Figure 1.[14]

Figure 1 shows that the main peak (t_R = 30 min), which accounted for 92.7% of the total UV area, was accompanied by earlier and later-eluting impurities. A sharp peak (t_R = 38.5 min, indicated by the arrow), which represented 0.8% of the total UV area, and whose characterization forms the main subject of this report, was also visible. Recently, we have shown that HPLC coupled to electrospray mass spectrometry (HPLC–MS) is a powerful tool for the routine analysis of therapeutic oligonucleotides.[15] The average mass spectrum of the t_R = 38.5 min impurity is shown in Figure 2.[14]

Keywords: Phosphorothioate oligonucleotides; Liquid chromatography–mass spectrometry; Universal solid support.
* Corresponding author. Tel.: +1 760 603 2532; fax: +1 760 603 4655; e-mail: dcapaldi@isisph.com

0960-894X/$ - see front matter © 2005 Elsevier Ltd. All rights reserved.
doi:10.1016/j.bmcl.2005.10.051

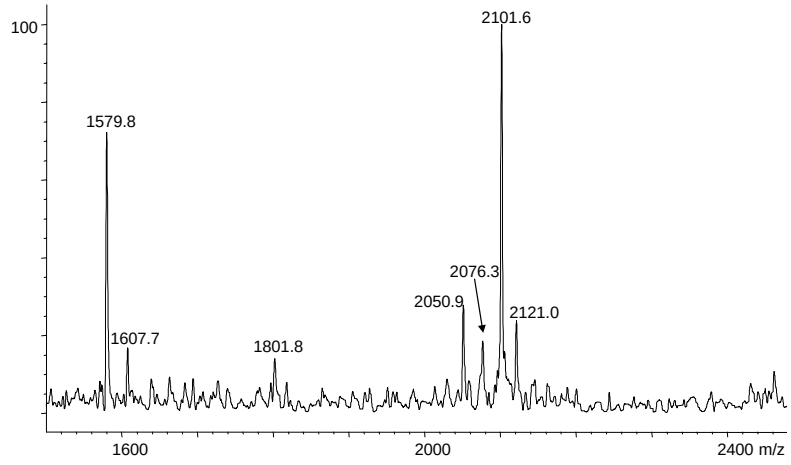

Figure 2. Average mass spectrum of t_R = 38.5 min component shown in Figure 1.

The spectrum contained signals that suggested the presence of several high molecular weight compounds. Due to their polyanionic nature, oligonucleotides are detected as multiply-charged species under electrospray ionization conditions, and often several charge states of the same molecule can be observed in any given analysis. Deconvoluting the different charge states allows one to determine the molecular weight. In the present case, the main signal at m/z = 2101.6, and another at m/z = 1801.8, were attributed to the negative (−) 6 and −7 charge states, respectively, of a component with a most abundant mass = 12,617.6 Da. Of the other signals observed, that at m/z = 1607.7 was present in all areas of the chromatogram following elution of the main UV peak and was attributed to the −4 charge state of the parent oligonucleotide. The signal at m/z = 1579.8 was likewise not associated with the t_R = 38.5 min component; this signal was observed at all retention times and was due to background levels of a tune component used to calibrate the mass spectrometer. Signals at m/z = 2050.9 and 2076.3, however, were unique to the t_R = 38.5 min region of the chromatogram. That these components eluted with the main 12,617.6 Da species indicated all three had approximately equivalent molecular weights and suggested the latter two were due to the −6 charge states of compounds with most abundant masses = 12,311.4 and 12,463.8 Da, respectively. Finally, although the signal at m/z = 2121.0 was present in this region of the chromatogram, it was much more pronounced under the broad peak at t_R = 37.8 min, where it was easily the most abundant ion present. By virtue of its retention time we assigned this signal to the −6 charge state of a component with a most abundant mass = 12,732.0 Da.

The most abundant mass of the main component of the t_R = 38.5 min peak (12,617.6 Da) was 251.6 Da less than twice that of parent oligonucleotide (2×6434.6 = 12,869.2 Da), a difference roughly equivalent to the mass of 2′-deoxyadenosine (252 Da). This observation led to the hypothesis that this component was an oligonucleotide of structure **1** or **2** (Chart 1).

We hypothesized that the main component of the peak at 38.5 min was an oligonucleotide comprised of a full-length molecule to which was attached a second oligonucleotide chain lacking its 3′-terminal-2′-deoxyadenosine residue. Compounds **1** and **2** differ in the site of attachment of the second chain. In **1**, this site is the exocyclic amino group of the 3′-terminal-2′-deoxyadenosine residue of the parent molecule; in **2**, it is its 3′-hydroxy group. The calculated most abundant mass for **1** and **2** is 12,618.1.[16] Similar structures were drawn to explain the masses of the minor components of the t_R = 38.5 min peak. Of these, the 12,463.8 Da component was an artifact formed by loss of guanine from the main component (calcd most abundant mass for **1** or **2** minus guanine = 12,467.0 Da). Its presence here was consistent with known fragmentation patterns of oligonucleotides.[17] The 12,311.4 Da, however, was real and we hypothesized that it was related to **1** or **2** by removal of the 3′-terminal-2′-deoxycytosine nucleotide from the shorter of the two chains (calcd most abundant mass for **1** or **2** minus dC_{PS} = 12,313.1 Da).

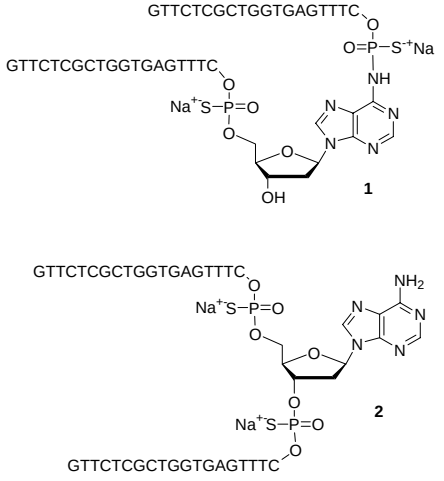

Chart 1. Potential structures of the t_R = 38.5 min impurity observed in ISIS 3521. All residues are 2′-deoxy and all internucleotide linkages are 3′-*O*,5′-*O* phosphorothioate diesters.

The third minor component of the t_R = 38.5 min peak, which was the major component of the t_R = 37.8 min peak (most abundant mass = 12,732.0 Da), did not

appear to be related to **1** or **2**. Instead its mass was consistent with that of a cross-linked oligonucleotide (e.g., Chart 2, **I**) formed by reaction of one molecule of ISIS 3521 with another molecule that had undergone depurination at its 3′-terminal-2′-deoxyadenosine residue (calcd most abundant mass = 12,734.1).

The formation of cross-linked species in the presence of depurinated oligonucleotides was described previously, although no structural information has been presented.[18] In this regard there are several points to consider about the structure proposed here. First, and most obviously, **I** is but one of the very many structures that might be drawn for a cross-linked oligonucleotide of the observed mass. Despite this ambiguity there are elements to **I** that are supported by results generated in this and other laboratories. First, we have demonstrated that in the presence of internally-located abasic sites, 2′-deoxycytidine residues react to form 6-(2-deoxy-β-D-*erythro*-pentofuranosyl)-3-(2-oxopropyl)imidazo[1,2-*c*]pyrimidin-5(6*H*)-one residues.[15c] This result provides some evidence for linking the strands at a cytosine residue. Presuming this is the case, one might imagine that reaction could take place at any of the cytosine residues of ISIS 3521 to produce a group of eight related components. The rather broad appearance of this peak suggests the presence of more than one component. A second piece of evidence supporting **I** was the fact that, while we were able to detect cross-linked components formed by reaction at abasic sites generated by loss of adenine, corresponding components formed by reaction at abasic sites generated by loss of guanine were absent, this despite the fact that ISIS 3521 contains low levels of both types of abasic site. This supports the hypothesis that cross-linked products form only through reaction at terminally located abasic sites (the 3′-terminal residue of ISIS 3521 is 2′-deoxyadenosine). This result was consistent with the susceptibility of internally located abasic sites and their Schiff bases toward strand cleavage,[19] and with our work indicating that reaction at internal abasic sites leads to oligonucleotides containing modified cytosine residues rather than cross-linked products.[15c] This second piece of evidence should be treated with some caution however, because, although ISIS 3521 may contain both internal and a 3′-terminally-located abasic sites, it is likely that the latter is the more abundant of the two.[20] In any event, formal identification of these apparently cross-linked components, including a determination of the nature of linkage between the two chains, will require additional investigation.

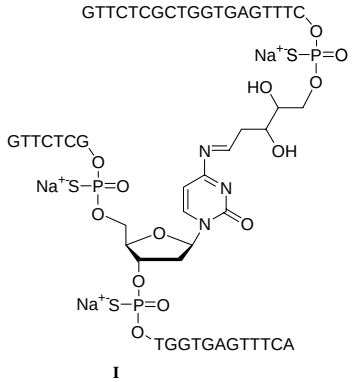

I

Chart 2. Examplary structure of a cross-linked oligonucleotide. All residues are 2′-deoxy and all internucleotide linkages are 3′-*O*,5′-*O* phosphorothioate diesters.

Returning to the identification of the major component of the t_R = 38.5 min impurity, we sought to provide evidence in support of structures **1** or **2**. Due to the size and complexity of this component our investigation began with the analysis of simpler model compounds. Our initial experiment consisted of performing a single solid phase synthetic cycle (detritylation, coupling, sulfurization, and capping) to add a 2′-deoxycytidine residue to a commercially available 5′-*O*-DMT-N^6-benzoyl-2′-deoxyadenosine-derivatized solid support.[21] The support-bound product was detritylated, deprotected, and cleaved from the solid support in the normal manner. Crude PS-d(CA) was analyzed by HPLC with UV and MS detection.[14] The HPLC–UV chromatogram (Fig. 3, upper panel) indicates, in addition to two large peaks (t_R = 20.3 and 20.9 min) attributable to the individual diastereoisomers of PS-d(CA), the presence of a later-eluting component (t_R = 30.1 min) that accounted for 1.3% of the total UV area. The average mass spectrum of this component (Fig. 3, lower panel) is consistent with the expected branched impurity of the parent dimer (**5** or **6**, Scheme 1, calcd. most abundant mass = 861.2 Da). Close inspection of the mass spectrum indicated the presence of two fragment ions, m/z = 555.0 and 439.0, the former consistent with loss of the 2′-deoxycytidine fragment shown, the latter with a fragment formed by cleavage of the glycosidic bond of the 2′-deoxyadenosine residue of **5**. In contrast to the m/z = 555.0 fragment, which can be generated from **5** or **6**, the m/z = 439.0 fragment is specific to the former.

With some evidence suggesting **5** as the more likely structure, we set out to prepare **5** and **6** by unambiguous means (Scheme 1), and to compare their chromatographic and spectral properties to those of the t_R = 30.1 min component present in crude PS-d(CA) (Fig. 3).

Synthesis of 5′-*O*-N^6-linked trimer **5** was accomplished using 5′-*O*-N^6-bis-DMT-protected 2′-deoxyadenosine-loaded support **3** and standard solid phase phosphoramidite techniques.[21] 3′,5′-*O*-Linked trimer **6** was synthesized using 3′,5′-*O*-di(dimethoxytrityl)-protected 2′-deoxyadenosine-loaded support **4**.[21] The crude products from each reaction were analyzed by HPLC with UV and MS detection (Fig. 4).[14]

The crude products from supports **3** and **4** are shown in Figures 4a and b, respectively. The crude product obtained from support **3** contained PS-d(CA) (t_R = 18.7 and 19.6 min) and a later-eluting peak (t_R = 31.4 min) that had a mass = 861.2 Da. The latter was isolated by preparative HPLC[21] and its structure was confirmed as trimer **5** by ^{31}P and ^{1}H and COSY NMR spectroscopy.[22] The product obtained from support **4** was cleaner, with trimer **6** (t_R = 32.6 min) accounting for 82% of the UV area. The UV chromatograms

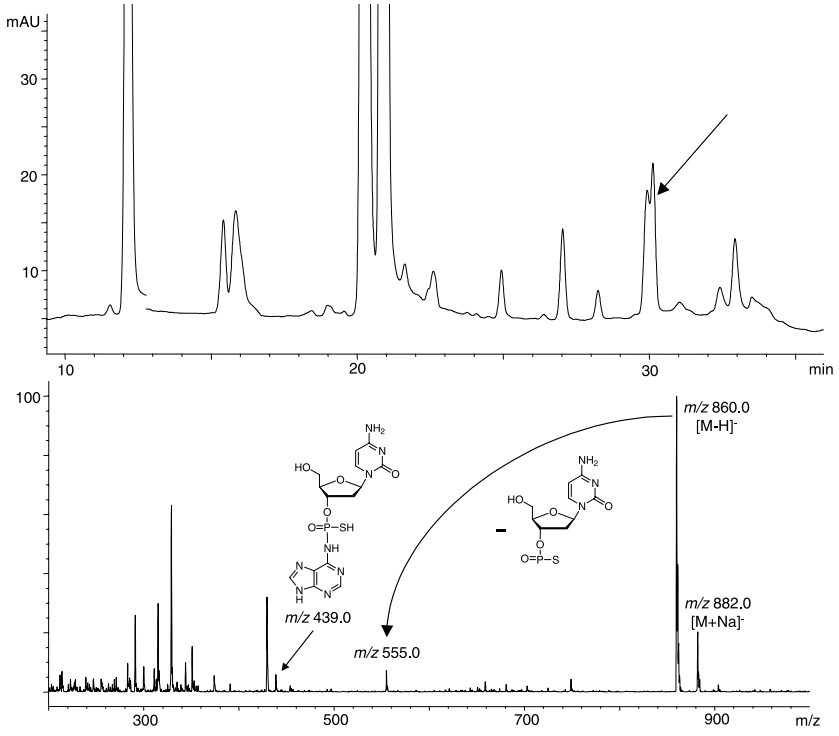

Figure 3. Upper panel: HPLC–UV chromatogram of PS-d(CA). Lower panel: average mass spectrum of t_R = 30.1 min component.

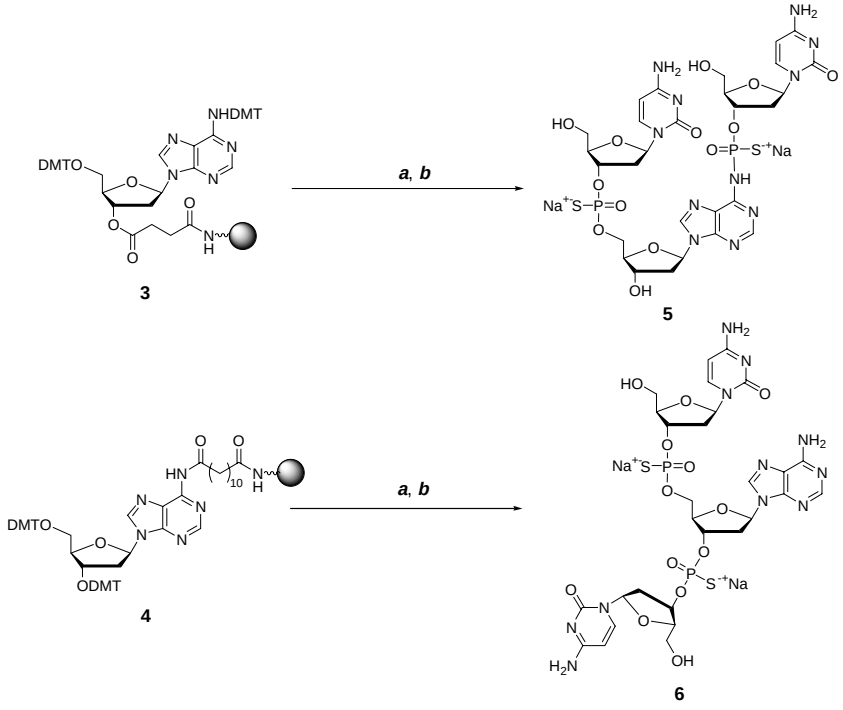

Scheme 1. Synthesis of trimers **5** and **6**. (a) Solid phase oligonucleotide synthesis; (b) ammonium hydroxide.

obtained by HPLC analysis of PS-d(CA) synthesized above on a commercially available 5′-*O*-DMT-N^6-benzoyl-2′-deoxyadenosine-derivatized solid support, and from analysis of a mixture of this material and the products of support **3**, are shown in Figures 4c and d, respectively. This analysis indicated that the impurity in PS-d(CA) and 5′-*O*-N^6-linked trimer **5** had the same retention time. In addition, the mass spectrum of **5** (data not shown) matched that shown in Figure 3, confirming the identity of the impurity in the synthesis of PS-d(CA) as 5′-*O*-N^6-linked trimer **5**.

Having established the identity of the impurity in PS-d(CA), we used support **3** in conjunction with standard

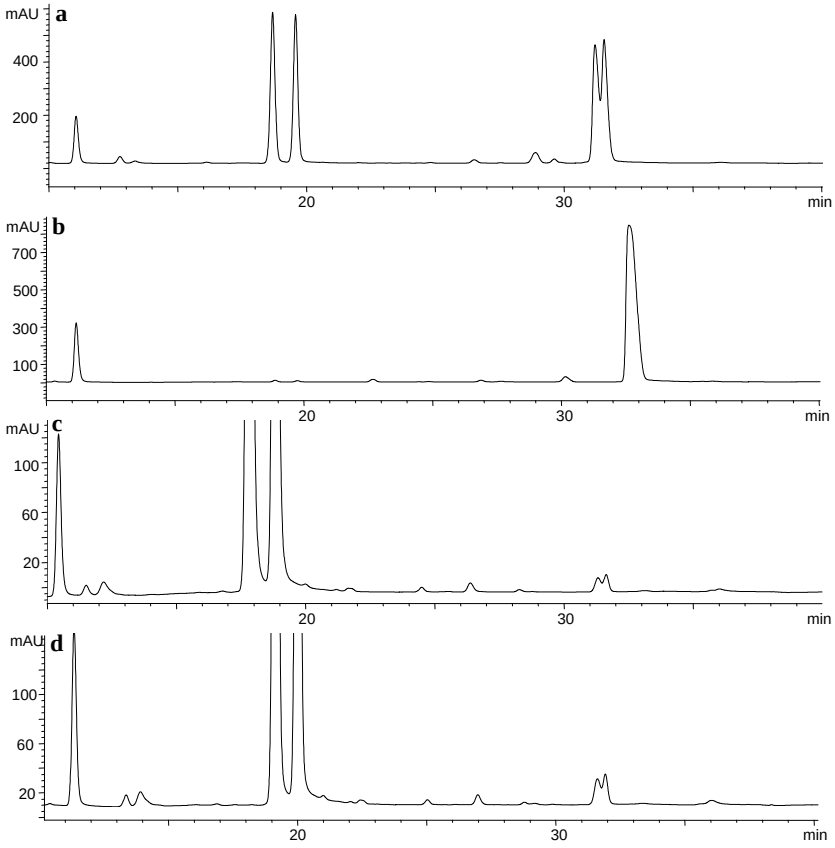

Figure 4. HPLC–UV chromatograms of (a) crude reaction mixture obtained from support **3**; (b) crude reaction mixture obtained from support **4**; (c) crude PS-d(CA); (d) mixture of (a) and (c).

solid phase oligonucleotide chemistry to synthesize oligonucleotide impurity **1**.[23] The HPLC–UV chromatogram and mass spectrum of HPLC-purified material are shown in Figures 5a and b, respectively.[14] The HPLC–UV chromatograms of ISIS 3521 drug substance and drug substance spiked with a small amount of **1** are shown in Figures 5c and d, respectively.

A comparison of Figure 5b with the mass spectrum of the $t_R = 38.5$ min impurity observed in ISIS 3521 (Fig. 2) indicates **1** and the impurity had identical mass spectral properties, while Figures 5c and d confirm the two have identical retention times. These results, in conjunction with those obtained using PS-d(CA) and trimer **5** above, provide strong evidence supporting our assignment of structure **1** to the $t_R = 38.5$ min impurity in ISIS 3521.

The formation of **1** in ISIS 3521 presumably occurs initially by reaction of 2′-deoxycytidine phosphoramidite with the 5′-hydroxyl and exocyclic amino groups of 2′-deoxyadenosine-loaded support. Further, it seems quite likely that reaction at the exocyclic amino group occurs because the benzoyl group that normally prevents reaction at this position is absent.[24] This mechanism suggests that if synthesis were conducted using a non-nucleoside support, oligonucleotides such as ISIS 3521 could be manufactured free of this type of impurity. A novel non-nucleoside linker suitable for large-scale manufacture of therapeutic-grade oligonucleotides was described recently.[25] In this approach, oligonucleotide synthesis is initiated by coupling the 3′-terminal residue to the hydroxyl group obtained by detritylation of *N*-phenyl-5-(4,4′-dimethoxytrityloxy)-6-hydroxy-4,7-epoxyhexahydroisobenzopyrrole-1,3-dione, itself attached to cross-linked polystyrene beads via a succinate ester spacer (Chart 3, **7**). Following synthesis and backbone deprotection, the crude product is released from the solid support by treatment with concentrated ammonium hydroxide. Under these conditions, the oxygen atom of the oxabicycloheptane ring system attacks the vicinal phosphorothioate diester linkage to produce the desired 3′-terminal hydroxyl group.

We examined the use of this support for its impact on levels of impurities of the type **1** in another oligonucleotide, ISIS 113715 (Chart 3, **8**).[26] Figure 6a shows the UV chromatogram of a batch of HPLC-purified **8** synthesized on 5′-*O*-DMT-N^4-benzoyl-2′-*O*-(2-methoxyethyl)-5-methylcytidine-loaded solid support.[14] The main UV component was accompanied by a set of later-eluting impurities ($t_R = 15.5$–18.3 min) that accounted for 3.0% of the total UV area. It should be noted that the broad peak (indicated by the arrow) was unique to this particular batch of drug substance and was not included in this estimate. The average mass spectrum of the $t_R = 15.5$–18.3 min portion of chromatogram is shown in Figure 6c. The mass spectrum[14] contained signals that were consistent with the presence of components of the type described above. Observed masses and proposed

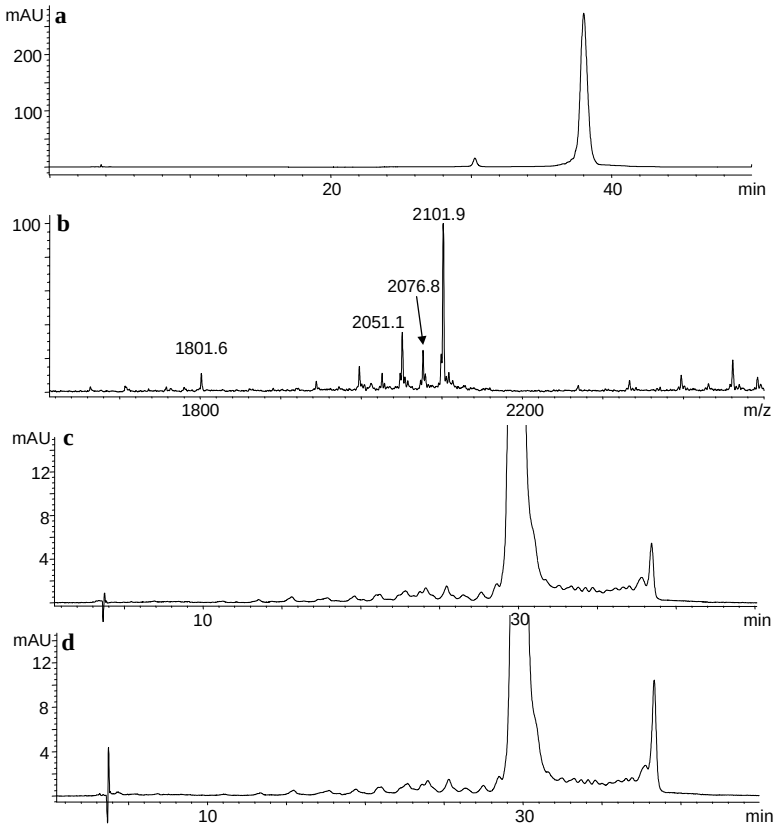

Figure 5. (a) HPLC–UV chromatogram of **1**; (b) average mass spectrum of main component (cf. with Fig. 2); (c) HPLC–UV chromatogram of ISIS 3521; (d) HPLC–UV chromatogram of a mixture of **1** and ISIS 3521.

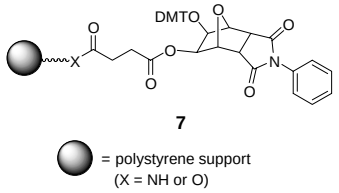

7

$\underline{G}^{Me}\underline{C}^{Me}\underline{U}\ {}^{Me}\underline{C}^{Me}\underline{C}T\ T^{Me}C^{Me}C\ A^{Me}CT\ GAT\ {}^{Me}\underline{C}^{Me}\underline{C}^{Me}\underline{U}\ \underline{G}^{Me}\underline{C}$

8

Chart 3. Structure of Unylinker derivatized solid support (**7**) and ISIS 113715 (**8**). In **8** the underlined are 2-(2-methoxyethyl)ribose residues; all others are 2-deoxyribose. All internucleotide linkages are 3′-*O*,5′-*O* phosphorothioate diesters.

structures and calculated masses for these components are given in Table 1.

As the data presented in Figure 6 and Table 1 indicate, impurities of the type **1** were present at much higher levels in **8** than in ISIS 3521. There are at least two potential explanations for this. First, it may be that support-bound 5-methyl-2′-*O*-(2-methoxyethyl)cytidine residues are more prone to benzoyl group loss than similarly protected, support-bound 2′-deoxyadenosine residues. While we know of no information comparing the stabilities of benzoylated cytidine and adenosine nucleosides attached to solid supports, the $t_{1/2}$s in ammonium hydroxide indicate the former are more labile than the latter.[27] Second, it might be that 5-methyl-2′-*O*-(2-methoxyethyl)cytidine is more reactive toward phosphitylation than 2′-deoxyadenosine. In this regard, Hayakawa and Katoaka have reported that with imidazolium triflate as activator, unprotected 2′-deoxycytidine phosphoramidites gave rise to twice as much N-phosphitylation as unprotected 2′-deoxyadenosine phosphoramidites.[24c]

The HPLC–UV chromatogram of purified **8**, synthesized using non-nucleoside support **7**, is shown in Figure 6b. It was evident that this material contained substantially lower levels of late eluting impurities than material made using nucleoside-loaded support (1.4% vs 3.0%) and indeed by mass spectrometry we were unable to detect the presence of any of the components listed in Table 1.

The data presented in this report indicate that phosphorothioate oligonucleotides synthesized using 2′-deoxyadenosine or 5-methyl-2′-*O*-(2-methoxyethyl)cytidine (and presumably 5-methyl-2′-deoxycytidine and 2′-deoxycytidine) derivatized solid supports can contain high molecular weight impurities of the type described. The problem appears more pronounced with 5-methyl-2′-*O*-(2-methoxyethyl)cytidine supports than with 2′-deoxyadenosine supports. It is likely that similar impurities arise during the synthesis of phosphate diester oligonucleotides. While it is certainly feasible that purification methods could be developed to remove these components, a more efficient approach might be to develop chemistries that avoid their formation. We have dem-

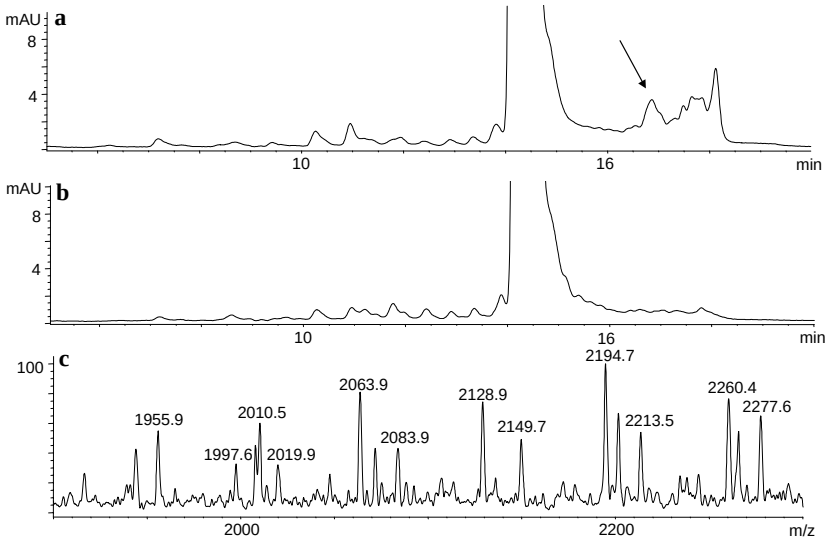

Figure 6. (a) HPLC–UV chromatogram of HPLC-purified **8** made with nucleoside-loaded support; (b) HPLC–UV chromatogram of HPLC-purified **8** made with Unylinker-loaded support; (c) average mass spectrum of t_R = 16–18.5 min region of HPLC chromatogram shown in (a).

Table 1. Observed masses, proposed structures, and calculated masses for components that elute between t_R = 15.5 and 18.3 min in Figure 6a

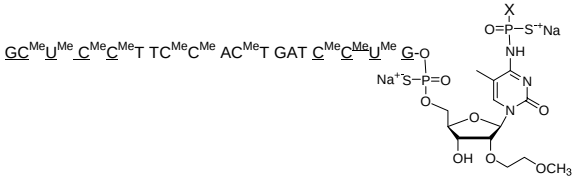

X*H*[a]	*m*/*z*	Charge state	Obsd most abundant mass (Da)	Calcd most abundant mass (Da)
G^{Me}C^{Me}U^{Me}C^{Me}CT T^{Me}C^{Me}C A^{Me}CT GAT^{Me}C^{Me}C^{Me}U G-O*H*	1997.6	−7	13,990.2	13,988.0
G^{Me}C^{Me}U^{Me}C^{Me}CT T^{Me}C^{Me}C A^{Me}CT GAT^{Me}C^{Me}C^{Me}U-O*H*	2260.4	−6	13,568.4	13,568.0
G^{Me}C^{Me}U^{Me}C^{Me}CT T^{Me}C^{Me}C A^{Me}CT GAT^{Me}C^{Me}C-O*H*	2194.7	−6	13,174.2	13,173.9
G^{Me}C^{Me}U^{Me}C^{Me}CT T^{Me}C^{Me}C A^{Me}CT GAT^{Me}C-O*H*	2128.9	−6	12,779.4	12,780.8
G^{Me}C^{Me}U^{Me}C^{Me}CT T^{Me}C^{Me}C A^{Me}CT GAT-O*H*	2063.9	−6	12,389.4	12,387.8
G^{Me}C^{Me}U^{Me}C^{Me}CT T^{Me}C^{Me}C A^{Me}CT GA-O*H*	2010.5	−6	12,069.0	12,066.7
G^{Me}C^{Me}U^{Me}C^{Me}CT T^{Me}C^{Me}C A^{Me}CT G-O*H*	1955.9	−6	11,741.4	11,737.7
G^{Me}C^{Me}U^{Me}C^{Me}CT T^{Me}C^{Me}C A^{Me}CT-O*H*	2277.6	−5	11,393.0	11,392.7
G^{Me}C^{Me}U^{Me}C^{Me}CT T^{Me}C^{Me}C A^{Me}C-O*H*	2213.5	−5	11,072.5	11,072.6
G^{Me}C^{Me}U^{Me}C^{Me}CT T^{Me}C^{Me}C A-O*H*	2149.7	−5	10,753.5	10,753.6
G^{Me}C^{Me}U^{Me}C^{Me}CT T^{Me}C^{Me}C-O*H*	2083.9	−5	10,424.5	10,423.6
G^{Me}C^{Me}U^{Me}C^{Me}CT T^{Me}C-O*H*	2019.9	−5	10,104.5	10,104.5

[a] Underlined are 2-(2-methoxyethyl)ribose residues; all others are 2-deoxyribose. All internucleotide linkages are 3′-*O*, 5′-*O* phosphorothioate diesters.

onstrated the realization of this second strategy through the use of the newly described Unylinker support.[25]

Acknowledgment

We thank Dr. Q. Song, Isis Pharmaceuticals, Inc. for acquiring NMR spectra of **5**.

Supplementary data

Supplementary data associated with this article can be found in the online version at doi:10.1016/j.bmcl.2005.10.051.

References and notes

1. Crooke, S. T. *Biochim. Biophys. Acta* **1999**, *1489*, 31.
2. Crooke, S. T. *Methods Enzymol.* **2000**, *313*, 3.
3. Crooke, S. T. *Antisense Drug Technology: Principles, Strategies, and Applications*; Marcel Dekker: New York, 2001.
4. In August 1998, Isis Pharmaceuticals Inc., Carlsbad, CA, and Ciba Vision, a division of Novartis AG, Switzerland, received FDA approval for Vitravene™ (fomivirsen sodium injectible) for the treatment of cytomegalovirus (CMV) retinitis. Several other phosphorothioate oligonucleotides are currently being evaluated in human clinical trials.
5. For a review see, Beaucage, S. L.; Iyer, R. P. *Tetrahedron* **1992**, *48*, 2223.

6. Cheruvallath, Z. S.; Carty, R. L.; Moore, M. N.; Capaldi, D. C.; Krotz, A. H.; Cole, D. L.; Ravikumar, V. T. *Org. Process Res. Dev.* **2000**, *4*, 199.
7. Capaldi, D. C.; Scozzari, A. N.; Cole, D. C.; Ravikumar, V. T. *Org. Process Res. Dev.* **1999**, *3*, 485.
8. Krotz, A. H.; Cole, D. L.; Ravikumar, V. T. *Bioorg. Med. Chem.* **1999**, *7*, 435.
9. Andrade, M.; Scozzari, A. N.; Cole, D. L.; Ravikumar, V. T. *Nucleosides Nucleotides* **1997**, *16*, 1617.
10. Capaldi, D. C.; Gaus, H.; Krotz, A. H.; Arnold, J.; Carty, R. L.; Moore, M. N.; Scozzari, A. N.; Lowery, K.; Cole, D. L.; Ravikumar, V. T. *Org. Process Res. Dev.* **2003**, *7*, 832.
11. Krotz, A. H.; McElroy, B.; Scozzari, A. N.; Cole, D. L.; Ravikumar, V. T. *Org. Process Res. Dev.* **2003**, *7*, 47.
12. Krotz, A. H.; Cole, D. L.; Ravikumar, V. T. *Nucleosides Nucleotides Nucleic Acids* **2003**, *22*, 129.
13. ISIS 3521 is an antisense inhibitor of PKC-α, a protein important for the growth of human cancers.
14. See Supplementary data for HPLC–UV and MS conditions.
15. (a) Capaldi, D. C.; Gaus, H. J.; Carty, R. L.; Moore, M. N.; Turney, B. J.; Decottignies, S. D.; McArdle, J. V.; Scozzari, A. N.; Ravikumar, V. T.; Krotz, A. H. *Bioorg. Med. Chem. Lett.* **2004**, *14*, 4683; (b) Gaus, H.; Olsen, P.; Van Sooy, K.; Rentel, C.; Turney, B.; Walker, K.; McArdle, J. V.; Capaldi, D. C. *Bioorg. Med. Chem. Lett.* **2005**, *15*, 4118; (c) Rentel, C.; Wang, X.; Batt, M.; Kurata, C.; Oliver, J.; Gaus, H.; Krotz, A. H.; McArdle, J. V.; Capaldi, D. C. *J. Org. Chem.* **2005**, *70*, 7841.
16. Most abundant masses were calculated using the Peptide Tools option located within Agilent's ChemStation© software package (Agilent Technologies, 1990–2001).
17. (a) McLuckey, S. A.; Habibi-Goudarzi, S. *J. Am. Chem. Soc.* **1993**, *115*, 12085; (b) Gut, I. V. *Int. J. Mass Spectrom. Ion Processes* **1997**, 313.
18. (a) Freese, E.; Cashel, M. *Biochim. Biophys. Acta* **1964**, *91*, 67; (b) Burnotte, J.; Verly, W. G. *Biochim. Biophys. Acta* **1972**, *262*, 449; (c) Goffin, C.; Bricteux-Gregoire, S.; Verly, W. G. *Biochim. Biophys. Acta* **1984**, *783*, 1; (d) Prakash, A. S.; Gibson, N. W. *Carcinogenesis* **1992**, *13*, 425.
19. Sugiyama, H.; Fujiwara, T.; Ura, A.; Tashiro, T.; Yamamoto, K.; Kawanishi, S.; Saito, I. *Chem. Res. Toxicol.* **1994**, *7*, 673.
20. Of the depurinated products of ISIS 3521, the 3′-terminally-located lesion is likely the most abundant because (a) the 3′-terminal 2′-deoxyadenosine residue is exposed to the detritylation conditions for every cycle of the synthesis and (b) a 3′-terminal lesion is more stable toward ammonium hydroxide treatment than an internal lesion.
21. See Supplementary data for the synthesis of PS-d(CA), supports **3** and **4**, and trimers **5** and **6**.
22. ^{1}H NMR [$(CD_3)_2SO$ containing D_2O] δ 8.68 and 8.64 (1H total, s), 8.39 (1H, s), 7.87 and 7.75 (2H, m) 6.46–6.42 (1H, m), 6.20–6.15 (2H, m), 5.82–5.76 (2H, m), 5.12–4.99 (1H, m), 4.87–4.74 (1H, m), 4.55–4.45 (1H, m), 4.19–3.83 (5H, m), ca. 3.67–3.43 (m, partially obscured by HOD), 2.82–2.68 (1H, m), 2.47–2.19 (3H, m), 2.09–1.86 (2H, m) ^{31}P NMR [$(CD_3)_2SO$] δ 53.86, 53.37, 43.88, 43.58 HRMS $[MH]^+$ Calcd for $C_{28}H_{37}N_{11}O_{13}P_2S_2$: 862.1562. Found: 862.1562.
23. See Supplementary data for the synthesis of oligonucleotide **1**.
24. The reaction of phosphoramidites with the exocyclic amino groups of adenine and cytosine residues has been described previously. For example, (a) Gryaznov, S. M.; Letsinger, R. L. *J. Am. Chem. Soc.* **1991**, *113*, 5876; (b) Wada, T.; Moriguchi, T.; Sekine, M. *J. Am. Chem. Soc.* **1994**, *116*, 9901; (c) Hayakawa, Y.; Katoaka, M. *J. Am. Chem. Soc.* **1998**, *120*, 12395; (d) Sekine, M.; Akihiro, O.; Kohji, S. *J. Org. Chem.* **2003**, *68*, 5478.
25. Scozzari, A., N. Presented at TIDES®, Boston, MA, May 2005.
26. ISIS 113715 is a chimeric, 2′-deoxy and 2′-(2-methoxyethyl)ribose, second-generation antisense inhibitor of protein tyrosine phosphatase 1-B (PTB-1B) that is being evaluated for the treatment of type 2 diabetes mellitus Zinker, B. A.; Rondinone, C. M.; Trevillyan, J. M.; Gum, R. J.; Clampit, J. E.; Waring, J. F.; Xie, N.; Wilcox, D.; Jacobson, P.; Frost, L.; Kroeger, P. E.; Reilly, R. M.; Koterski, S.; Opgenorth, T. J.; Ulrich, R. G.; Crosby, S.; Butler, M.; Murray, S. F.; McKay, R. A.; Bhanot, S.; Monia, B. P.; Jirousek, M. R. *PNAS* **2002**, *99*, 11357.
27. $t_{1/2}$s in concentrated ammonium hydroxide at 20 °C for N^6-benzoyl-2′-deoxyadenosine and N^4-benzoyl-2′-deoxycytidine are reported to be 8 and 2 h, respectively, Schulhof, J. C.; Molko, D.; Teoule, R. *Nucleic Acids Res.* **1987**, *15*, 397.